

## Partonic distributions for large $x$ and renormalization of Wilson loop \*

G. P. KORCHEMSKY<sup>† ‡</sup> and G. MARCHESINI

*Dipartimento di Fisica, Università di Parma and  
INFN, Gruppo Collegato di Parma, I-43100 Parma, Italy*

### Abstract

We discuss the relation between partonic distributions near the phase space boundary and Wilson loop expectation values calculated along paths partially lying on the light-cone. Due to additional light-cone singularities, multiplicative renormalizability for these expectation values is lost. Nevertheless we establish the renormalization group equation for the light like Wilson loops and show that it is equivalent to the evolution equation for the physical distributions. By performing a two-loop calculation we verify these properties and show that the universal form of the splitting function for large  $x$  originates from the cusp anomalous dimension of Wilson loops.

---

\*Research supported in part by Ministero dell'Universtà e della Ricerca Scientifica e Tecnologica.

<sup>†</sup>On leave from the Laboratory of Theoretical Physics, JINR, Dubna, Russia

<sup>‡</sup>INFN Fellow

# 1. Introduction

It is well known [1] that for hard distributions such as deep inelastic structure functions, fragmentation functions, Drell-Yan pair cross section, jet production etc. near the phase space boundary the perturbative expansion involves large corrections which needed to be summed [2, 3]. This region is characterized by the presence of two large scales  $Q^2$  and  $M^2$  with  $Q^2 \gg M^2 \gg \Lambda_{\text{QCD}}^2$  and at any order in perturbation theory the leading contributions are given by double logarithmic terms ( $\alpha_s^n \ln^{2n} Q^2/M^2$ ). The leading contributions can be summed and the result is given by the exponentiation of the one-loop contribution [4]. This exponentiated form holds also after the summation of the next-to-leading contributions ( $\alpha_s^n \ln^{2n-1} Q^2/M^2$ ). The exponent is simply modified by two-loop corrections in which the term  $\alpha_s^2 \ln^4 Q^2/M^2$  is absent and the coefficient of  $\alpha_s^2 \ln^3 Q^2/M^2$  is proportional to the one-loop beta-function [5]. This fact suggests us to apply renormalization group approach for summing large perturbative contributions to all orders.

The universal properties of hard processes near the phase space boundary originate from the universality of soft emission, which is responsible of the double logarithmic contributions. Soft gluon emission from fast quark line can be treated by eikonal approximation for both incoming and outgoing quarks. In the eikonal approximation quarks behave as classical charged particles and their interaction with soft gluons can be described by path ordered Wilson lines along their classical trajectories [6, 7]. The corresponding hard distribution is then given by the vacuum averaged product of the time-ordered Wilson line, corresponding to the amplitude, and the anti-time ordered Wilson line, corresponding to the complex conjugate amplitude. The combination of these Wilson lines forms a path ordered exponential  $W(C)$  along a closed path  $C$  which lies partially on the light-cone and depends on the kinematic of the hard process

$$W(C) \equiv \langle 0 | \mathcal{P} \exp \left( ig \oint_C dz_\mu A^\mu(z) \right) | 0 \rangle, \quad A_\mu(z) = A_\mu^a(z) \lambda^a \quad (1.1)$$

where  $\lambda^a$  are the gauge group generator. Here the gluon operators are ordered along the integration path  $C$  and not according to time. Notice that on different parts of the path  $C$  the gluon fields are time or anti-time ordered. This expression is different from the usual Wilson loop expectation value in which one has ordering along the path for the colour indices of  $\lambda^a$  and ordering in time for the gluons fields  $A_\mu^a(z)$ . In eq. (1.1) we have ordering both of colour matrices and gauge fields along the path.

In this paper we study the renormalization properties of  $W(C)$  for a path  $C$  partially lying on the light-cone and show that renormalization group (RG) equation for  $W(C)$  corresponds to the evolution equation [8] for the parton distribution function or the fragmentation function near the phase space boundary. In particular, we discuss the relation between the ‘‘cusp anomalous dimension’’ of Wilson loop and the splitting function  $P(z)$  for  $z \rightarrow 1$ .

In sect. 2 we establish the relation between  $W(C)$  and the distribution function or fragmentation function near the phase space boundary. In sect. 3 we perform the two-loop calculation in the Feynman gauge and in the  $\overline{\text{MS}}$ -regularization scheme of  $W(C)$  with the path  $C$  fixed by the kinematics of hard process. In sect. 4 we deduce the RG equation for  $W(C)$  and show in sect. 5 that this equation gives rise to the evolution equation for the distribution function and fragmentation function near the phase space boundary. Sect. 6 contains some concluding remarks.

## 2. Wilson loop and structure function in the soft limit

Consider the deep inelastic process for an incoming hadron of energy  $E$ , longitudinal momentum  $P_\ell$  and mass  $M$  probed by a hard photon with momentum  $q$ . In the infinite momentum frame we have  $P_+ \gg P_-$ , where the light-cone variables for the hadron momentum  $P_\mu = (P_+, \mathbf{P}_T, P_-)$  are defined by

$$P_+ = (E + P_\ell)/\sqrt{2}, \quad P_- = (E - P_\ell)/\sqrt{2}, \quad \mathbf{P}_T = (P_1, P_2) = 0.$$

In this frame  $xP_+$  is the “+” component of the momentum of the quark probed by the hard photon, where  $x = -q^2/2(P \cdot q)$  is the Bjorken variable. For  $x \rightarrow 1$  the hard photon probes at short distances the quark which carries nearly all hadron momentum. In this region the hard process is characterized by two scales: the virtuality of the photon  $Q^2 = -q^2$ , which gives the short distance scale, and the large distance scale  $(1-x)Q^2$ .

In this Section we show that, after factorization of leading twist contributions, the partonic distributions for  $x \rightarrow 1$  are given in terms of a generalized Wilson loop in (1.1). To show this we first make the leading twist approximation and then we perform the  $x \rightarrow 1$  limit.

### 2.1. Summing collinear gluons

Due to the factorization theorem [9] the differential cross-section of this process is given in terms of the partonic distribution function and the partonic cross section. The partonic distribution function is a universal distribution measuring the probability to find in the hadron a parton with  $x$  fraction of the  $P_+$  momentum. To leading twist ( $Q^2 \gg M^2$ ) the quark distribution function has the following representation [10]

$$F(x, \mu/M) = \int_{-\infty}^{+\infty} \frac{dy_-}{2\pi} e^{-iP_+ y_- x} \langle P | \bar{\Psi}(y) \mathcal{P} \exp \left( ig \int_0^y dz_\mu A^\mu(z) \right) \gamma_+ \Psi(0) | P \rangle, \quad (2.1)$$

where the vector  $y_\mu$  lies on the light-cone with components

$$y_\mu = (y_+, \mathbf{y}_T, y_-) = (0, \mathbf{0}, y_-).$$

The state  $|P\rangle$  describes the hadron with momentum  $P$  and mass  $M$ . Integration over  $y_-$  fixes the value of the “+” component of the total momentum of the emitted radiation to be  $(1-x)P_+$ . The corresponding transverse and “-” components are integrated over by fixing  $\mathbf{y}_T = 0$  and  $y_+ = 0$ . Because of these unrestricted integrations the structure function contains ultraviolet (UV) divergences which are subtracted at the reference point  $\mu$ . The quark field operators  $\bar{\Psi}(y)$  and  $\Psi(0)$  are defined in the Heisenberg representation. The path ordered exponential is evaluated along the line between points 0 and  $y_\mu$  on the light-cone and ensures the gauge invariance of the nonlocal composite quark–antiquark operator.

In what follows we will intensively use properties of Wilson lines which will appear in our analysis. We now briefly describe the physical meaning of Wilson line entering into the definition (2.1). Let us start considering the general form of the structure function of the deep inelastic scattering as matrix element of two electromagnetic currents:

$$\int \frac{d^4 z}{(2\pi)^4} e^{-iqz} \langle P | j_+(z) j_+(0) | P \rangle, \quad (2.2)$$

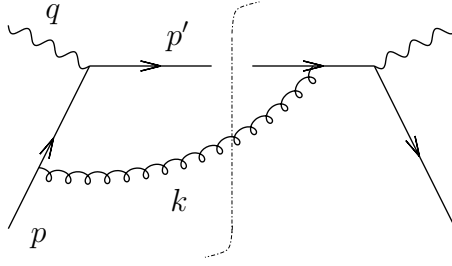


Figure 1: One-loop Feynman diagram contributing to the structure function of deep inelastic scattering. The gluon with momentum  $k$  is emitted by the quark  $p$  and absorbed by the quark  $p'$  in the final state. We use solid line for quarks, curly lines for gluons, wavy lines for photons and dot-dashed line for the unitary cut.

where

$$j_\mu(z) = \bar{\Psi}(z)\gamma_\mu\Psi(z).$$

It is well known that in the leading twist approximation the structure function is defined by contributions of Feynman diagrams in which only one of the quarks of the hadron  $|P\rangle$  participates in the hard scattering<sup>§</sup>. One of these diagrams is shown in fig. 1. In the infinite momentum frame, in the leading twist limit one can neglect the transverse motion of the quark inside the hadron and put the velocity of quark equal to the hadron velocity,

$$v_\mu = P_\mu/M. \quad (2.3)$$

As we will show in sect. 3, all singularities of the distribution function for  $x \rightarrow 1$  are absorbed by Wilson loop depending on the quark velocity  $v$  rather than momentum.

Consider for example the one-loop contribution of fig. 1 to (2.2). In the infinite momentum frame the incoming quark has momentum  $p_\mu$  with  $p_- \ll p_+$  whereas the recoiling momentum  $P'$  has component  $p'_- \gg p'_+$ . The vertices for the absorption and emission of the real gluon  $k$  are given by

$$\frac{\not{p}\gamma_\mu(\not{p}-\not{k})}{-2pk+i0} \quad \text{and} \quad \frac{\not{p}'\gamma_\mu(\not{p}'+\not{k})}{2p'k-i0}$$

respectively. For vanishing quark mass the two vertices contain the following singularities:

- $p$ -collinear:  $k_+ \sim p_+$ ,  $k_- \sim p_-$
- $p'$ -collinear:  $k_+ \sim p'_+$ ,  $k_- \sim p'_-$
- soft:  $k_- \sim k_+ \rightarrow 0$ ,

with  $\mathbf{k}_T^2 = 2k_+k_-$ . According to the LNK theorem [11], by summing all diagrams for the structure function both the  $p'$ -collinear and the soft (or infrared) singularities cancel. We then focus our attention only on the  $p$ -collinear singularities. There are also diagrams with quark-photon vertices “dressed” by hard virtual gluons and quarks having momentum  $k_+, k_-, k_T \sim Q$ . The contribution of hard virtual subprocesses can be factorized into the partonic cross section.

<sup>§</sup>There are also contributions initiated by gluons. The corresponding Feynman diagrams necessary involve real emitted quarks whose contribution is suppressed for  $x \rightarrow 1$ .

Consider the vertex for the absorption of gluon  $k$  with gauge potential  $a_\mu(k)$  in the momentum representation

$$g \frac{\not{p}' \not{k} (\not{p}' + \not{k})}{2p'k - i0}, \quad (2.4)$$

where the gluon field carries longitudinal and transverse polarizations. It can be easily shown that when the momentum  $k$  is collinear to  $p$ , the components of  $a_\mu(k)$  transverse to  $k$  contribute to higher twist and can be neglected. Thus, only longitudinal polarization survives and the gauge potential becomes pure gauge field

$$a_\mu(k) = k_\mu \left( \frac{y a(k)}{yk - i0} \right).$$

This property allows us to sum to all orders the contribution of collinear gluons (leading twist approximation) using Ward identities. Inserting this gauge field in (2.4) we obtain that the gluon emission is factorized into

$$\not{p}' \cdot g \int \frac{d^4 k}{(2\pi)^4} \left( \frac{y a(k)}{yk - i0} \right) = \not{p}' \cdot ig \int d^4 x J_\mu(x) A^\mu(x) = \not{p}' \cdot ig \int_0^\infty d\tau y_\mu A^\mu(y\tau), \quad (2.5)$$

where

$$J_\mu(x) = y_\mu \int_0^\infty d\tau \delta^4(x - y\tau)$$

is the classical non-abelian eikonal current of the scattered quark  $p'$  in which we neglect higher twists contributions of order  $p'_+/p'_-$ . This factorization property implies that the quark field operator  $\bar{\Psi}(0)$  describing the scattered quark  $p'$  in (2.2) can be written in one-loop as

$$\bar{\Psi}(0) = \bar{\Psi}_0(0) \left( 1 + ig \int_0^\infty dz_\mu A^\mu(z) + \mathcal{O}(g^2) \right) \quad (2.6)$$

with integration path along  $y_-$  axis. Here,  $\bar{\Psi}_0(0)$  is a free quark operator and  $A^\mu(x)$  describes  $p$ -collinear gluon. Note that this relation is valid only within the matrix element of currents in (2.2) and not as an operator identity.

The generalization of the one loop result (2.6) is based on the following physical arguments. After the hard scattering the quark with momentum  $p'$  starts to emit gluons and quarks moving in the same direction. All these particles form  $p'$ -collinear jet propagating through the cloud of  $p$ -collinear gluons created by the incoming quark. Since  $p$ -collinear gluons are pure gauge fields they cannot change the state of the scattering quark but only modify its phase. Such a pure phase factor is given by Wilson line along the light-cone direction  $y$  defined in (2.1). The generalization of (2.6) is then

$$\bar{\Psi}(0) = \bar{\Psi}_{p'\text{-col}}(0) \Phi_y[0, \infty; A], \quad (2.7)$$

where  $\Phi_y(z_1, z_2)$  is the path ordered exponential calculated from point  $z_1$  to  $z_2$  along the direction  $y$

$$\Phi_y[z_1, z_2; A] \equiv \mathcal{P} \exp \left( ig \int_{z_1}^{z_2} dz_\mu A^\mu(z) \right).$$

In (2.7) the phase  $\Phi_y[0, \infty; A]$  describes the interaction of  $p$ -collinear gluons with the scattered quark while operator  $\bar{\Psi}_{p'\text{-col}}(0)$  describes the jet of  $p'$ -collinear particles produced by the scattered quark.

For the quark field operator  $\Psi(z)$ , which describes absorption of  $p$ -collinear gluons by quark with momentum  $p'$  in the final state, one obtains

$$\Psi(z) = \Phi_{-y}[\infty, y; A] \Psi_{p'-\text{col}}(z), \quad (2.8)$$

with  $y = (0, \mathbf{0}, y_-)$  and  $y_- = z_-$ . After substitution of (2.7) and (2.8) into (2.2) we get that the full phase of the scattered quark is given by

$$\Phi_{-y}[\infty, y; A] \Phi_y[0, \infty; A] = \mathcal{P} \exp \left( ig \int_0^y dz_\mu A^\mu(z) \right). \quad (2.9)$$

Moreover, the contributions of  $p$ -collinear and soft particles to the structure function can be factorized into the distribution function (2.1). The contribution of  $p'$ -collinear jet is factorized as usual into the partonic cross section <sup>¶</sup>. Thus, the Wilson line in the definition of the distribution function (2.1) is the result of the interaction of scattered quark  $p'$  with the gluons collinear to incoming quark  $p$ . Here, we have used the following properties of the Wilson lines:

$$\begin{aligned} \bullet \text{ hermiticity:} & \quad \Phi_y^\dagger[0, \infty; A] = \Phi_{-y}[\infty, 0; A] \\ \bullet \text{ causality:} & \quad \Phi_y[b, c; A] \Phi_y[a, b; A] = \Phi_y[a, c; A] \\ \bullet \text{ unitarity:} & \quad \Phi_y^\dagger[a, b; A] \Phi_y[a, b; A] = 1 \end{aligned} \quad (2.10)$$

Notice, that the approximation (2.9) is valid in the leading twist limit for an arbitrary values of the scaling variable  $x$ .

## 2.2. Soft approximation for $x \rightarrow 1$

For  $x \rightarrow 1$  the total “+” momentum of the emitted radiation  $(1-x)P_+$  vanishes and the expression (2.1) can be further simplified. In the leading twist order only  $p$ -collinear and soft gluons contribute to (2.1). As already recalled, due to the LNK theorem  $p$ -collinear singularities survive in parton distribution (2.1). Although soft divergences cancel, their finite contribution completely determines the asymptotic parton distribution function for  $x \rightarrow 1$ . To show this we observe that for  $x \rightarrow 1$ , the “+” component of the momentum of any emitted *real* gluon  $q$  is positive and vanishing as  $q_+ \sim (1-x)P_+$ . Therefore,  $p$ -collinear gluons are only virtual since their momentum  $q$  has component  $q_+ \sim P_+$ . It means that real emitted gluons are only soft (with momenta  $q_+, q_-, q_T \sim (1-x)P_+$ ) while virtual gluons can be either soft or  $p$ -collinear.

These conditions imply that before hard scattering by photon probe, the incoming quark with momentum  $p$  decays into a jet of  $p$ -collinear virtual gluons and quarks emitting and absorbing soft gluons. The contribution of real and virtual soft gluons can be factorized from the distribution function as follows. We note that soft gluons interact with the  $p$ -collinear quarks and gluons, forming the  $p$ -collinear jet, via eikonal vertices. In this approximation the incoming quark with momentum  $p$  behaves as a classical charged particle moving with velocity  $v_\mu$  defined in (2.3) and all effects of interaction of the  $p$ -collinear jet produced by incoming quark with soft gluons are absorbed into phase factors similar to path-ordered exponentials found in the collinear

---

<sup>¶</sup>As notices in refs. [2, 3], the latter contribution become large for  $x \rightarrow 1$ . That is why performing the factorization of the structure function for  $x \rightarrow 1$  one should treat the  $p'$ -collinear jet separately from the partonic cross section.

approximation. Therefore, in the  $x \rightarrow 1$  limit one can replace quark field operators in the definition (2.1) as

$$\bar{\Psi}(y) = \bar{\Psi}_{p\text{-col}}(y)\Phi_{-v}[y, \infty; A], \quad \Psi(0) = \Phi_v[\infty, 0; A]\Psi_{p\text{-col}}(0), \quad (2.11)$$

where the phase factors are evaluated along a trajectory of a massive classical particle with velocity  $v$ . Here, the gauge field operators  $A_\mu(x)$  describe soft gluons and the quark fields  $\bar{\Psi}_{p\text{-col}}(y)$  and  $\Psi_{p\text{-col}}(0)$  describe the incoming quark in the initial and final states dressed by  $p$ -collinear virtual corrections.

We did not consider till now the contribution of quark emissions to the distribution function. Repeating the previous arguments one finds that for  $x \rightarrow 1$  *real* quarks are soft. But it is well known from power counting [12] that soft quarks give vanishing contribution to the leading twist order. Therefore all emitted quarks must be virtual and they contribute either to  $p$ -collinear jet or renormalize soft gluon self-interaction vertices. These last contributions will be explicitly evaluated in subsect. 3.2.

It should be noticed that similar phase factors (2.7) and (2.8) describe interaction of scattered quark with  $p$ -collinear gluons and incoming quark with soft gluons, respectively, although the two subprocesses are different. This is due to the fact that in both cases gluons do not change the quark state: the collinear gluons are pure gauge fields with vanishing strength; the soft gluons interact with quarks via eikonal vertices which preserve the momentum and polarization of the quarks.

Combining the phase factors (2.9) and (2.11) from collinear and soft approximations we obtain the following representation for the distribution function in the  $x \rightarrow 1$  limit:

$$F(x, \mu/M) = H(\mu/M) \int_{-\infty}^{+\infty} P_+ \frac{dy_-}{2\pi} e^{iP_+ y_- (1-x)} W(C_S) \quad (2.12)$$

with the function  $H(\mu/M)$  taking into account contributions of  $p$ -collinear quarks and gluons and

$$W(C_S) = \langle 0 | \Phi_{-v}[y, \infty; A] \Phi_y[0, y; A] \Phi_v[\infty, 0; A] | 0 \rangle \equiv \langle 0 | \mathcal{P} \exp \left( ig \oint_{C_S} dz_\mu A^\mu(z) \right) | 0 \rangle, \quad (2.13)$$

where the index  $S$  indicates that the photon probe has space-like momentum. The integration path  $C_S = \ell_1 \cup \ell_2 \cup \ell_3$  is shown in fig. 2. The rays  $\ell_1$  and  $\ell_3$  correspond to two classical trajectories of a massive particle going from infinity to 0 with velocity  $v$  and from  $y$  to infinity with velocity  $-v$ , respectively. The segment  $\ell_2 = [0, y]$  lies on the light-cone. As explained before, since we are dealing with a cross-section rather than with an amplitude, the gauge fields are ordered along the path rather than the time. Path- and time-orderings are related as follows

$$\mathcal{P} = \mathcal{T} \text{ for } \ell_1, \quad \mathcal{P} = \bar{\mathcal{T}} \text{ for } \ell_3, \quad \mathcal{P} = \mathcal{T} \text{ for } \ell_2 \text{ and } y_- > 0, \quad \mathcal{P} = \bar{\mathcal{T}} \text{ for } \ell_2 \text{ and } y_- < 0,$$

where  $\mathcal{T}$  and  $\bar{\mathcal{T}}$  denote time- and anti-time ordering, respectively. This path has two cusps at the points 0 and  $y$  where the direction of the particle is changed by the hard photon probe.

Thus the quark distribution function for  $x \rightarrow 1$  is given by the product of two functions: the Fourier transform of the Wilson loop expectation value, which takes into account all soft emissions and gives the asymptotic distribution function for  $x \rightarrow 1$ , and times the function  $H(\mu/M)$  getting contribution from virtual  $p$ -collinear quarks and gluons. This is the reason why  $H(\mu/M)$  does not depend on  $P_+(1-x)$  or, equivalently, on  $y_-$ . Although  $F(x, \mu/M)$  cannot be calculated in perturbation theory we will find its evolution with the renormalization point  $\mu$  using renormalization properties of  $W(C_S)$ .

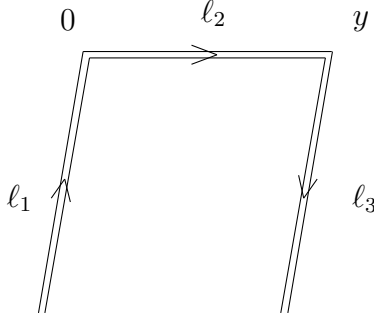


Figure 2: Integration path  $C_S = \ell_1 \cup \ell_2 \cup \ell_3$  for the Wilson loop  $W(C_S)$  corresponding to the structure function for large  $x$ . The ray  $\ell_1$  is along the time-like vector  $v_\mu$  from  $-\infty$  to 0; the segment  $\ell_2$  is from point 0 to  $y$  along the light-cone; the ray  $\ell_3$  is from the point  $y$  to  $-\infty$  along the vector  $-v_\mu$ . This path has two cusps at points 0 and  $y$  where the quark undergoes hard scattering.

### 2.3. Fragmentation function in the $x \rightarrow 1$ limit

The Wilson loop representation for the structure function in (2.12) can be easily generalized for the fragmentation function  $D(x, \mu/M)$  in the limit  $x \rightarrow 1$ . This function gives the probability of finding a hadron in a quark jet. To the leading twist approximation the fragmentation function is given by [10]

$$D(x, \mu/M) = \int_{-\infty}^{+\infty} \frac{dy_-}{2\pi} e^{-iP_+ y_- / x} \sum_f \langle P, f | \bar{\Psi}(y) \Phi_y[\infty, y; A] | 0 \rangle \gamma_+ \langle 0 | \Phi_{-y}[0, \infty; A] \Psi(0) | P, f \rangle \quad (2.14)$$

where  $P_\mu = (P_+, \mathbf{0}, P_-)$  is momentum of the observed hadron,  $y = (0, \mathbf{0}, y_-)$  is a vector in coordinate space which lies on the light-cone, and  $f$  denotes the associated final state radiation. In the infinite momentum frame with  $P_+ \gg P_-$  integration over  $y_-$  fixes the “+” component of the total associated radiation momentum to be  $(1/x - 1)P_+$ . As in Subsection 2.1, the phase factors in eq.(2.14) are obtained from the resummation of gluons interacting with the recoiling quark  $P'$  and collinear to the observed hadron  $P$ .

In the limit  $x \rightarrow 1$  the associated radiation becomes soft and we can perform the eikonal approximation as in the previous section. Namely, the dependence of gauge fields in the quark and anti-quark field operators in (2.14) factorizes into two phase factors as in eq.(2.11). In the soft ( $x \rightarrow 1$ ) limit we obtain the following representation for the fragmentation function

$$D(x, \mu/M) = H(\mu/M) \int_{-\infty}^{+\infty} P_+ \frac{dy_-}{2\pi} e^{iP_+ y_- (1-1/x)} W(C_T).$$

The generalized vacuum averaged Wilson loop operator  $W(C_T)$  is given by

$$\begin{aligned} W(C_T) &= \sum_f \langle f | \Phi_v[y, \infty; A] \Phi_y[\infty, y; A] | 0 \rangle \langle 0 | \Phi_{-y}[0, \infty; A] \Phi_{-v}[\infty, 0; A] | f \rangle \\ &= \langle 0 | \Phi_v[y, \infty; A] \Phi_y[0, y; A] \Phi_{-v}[\infty, 0; A] | 0 \rangle \\ &\equiv \langle 0 | \mathcal{P} \exp \left( ig \oint_{C_T} dz_\mu A^\mu(z) \right) | 0 \rangle, \end{aligned}$$



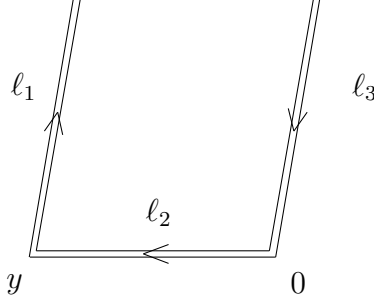


Figure 3: Integration path  $C_T$  corresponding to the fragmentation function for large  $x$ .

where we have used completeness condition for the associated radiation  $1 = \sum_f |f\rangle\langle f|$  and causality (2.10) for the phase factors. The index  $T$  indicates that the photon probe has time-like momentum.

The integration path  $C_T = l_1 \cup l_2 \cup l_3$  is shown in fig. 3 and three parts  $l_i$  have meanings similar to that described before for the space-like process. In this case path- and time-orderings are related as follows

$$\mathcal{P} = \mathcal{T} \text{ for } l_1, \quad \mathcal{P} = \bar{\mathcal{T}} \text{ for } l_3, \quad \mathcal{P} = \mathcal{T} \text{ for } l_2 \text{ and } y_- > 0, \quad \mathcal{P} = \bar{\mathcal{T}} \text{ for } l_2 \text{ and } y_- < 0$$

This path has two cusps at the points 0 and  $y$  where the direction of the particle is changed by the hard photon probe.

## 2.4. One-loop calculation

We perform the one-loop calculation of  $W(C_S)$  in order to explain in this formulation the nature and origin of double logarithms and to discuss the analytical properties of  $W(C_S)$  in the  $y_-$  variable.

We parameterize the integration path  $C_S = l_1 \cup l_2 \cup l_3 = \{z_\mu(t); t \in (-\infty, +\infty)\}$  as follows

$$z_\mu(t) = \begin{cases} v_\mu t, & -\infty < t < 0 \\ y_\mu t, & 0 < t < 1 \\ y_\mu - v_\mu(t-1), & 1 < t < \infty \end{cases}, \quad v_\mu \equiv \frac{P_\mu}{M}.$$

The relevant diagrams are given in fig. 4 plus the symmetric ones. We perform the calculation in the Feynman gauge and in coordinate representation by using the dimensional regularization. As we shall see in the sect. 3 this representation is very convenient for the calculation of  $W(C_S)$  to two loops. Feynman rules in coordinate representation are summarized in the Appendix A.

The path from point 0 to  $y$  consists actually of the product of paths from 0 to  $\infty$  and from  $\infty$  to  $y$  as shown in fig. 5 for the diagram of fig. 4a. The gluon is either real (fig. 5a) or virtual (fig. 5b). In both cases the gluon is emitted at point  $z_1 = vt_1$  with  $t_1 < 0$ . For real gluon we have  $z_2 = yt_2$  with  $1 < t_2 < \infty$ , while for virtual gluon we have  $z_2 = yt_2$  with  $0 < t_2 < \infty$ . The two contributions are given by

$$W_a^{(1)} = (ig)^2 C_F v_\mu y_\nu \int_{-\infty}^0 dt_1 \left\{ \int_0^\infty dt_2 D^{\mu\nu}(z_2 - z_1) + \int_\infty^1 dt_2 D_+^{\mu\nu}(z_2 - z_1) \right\} \quad (2.15)$$

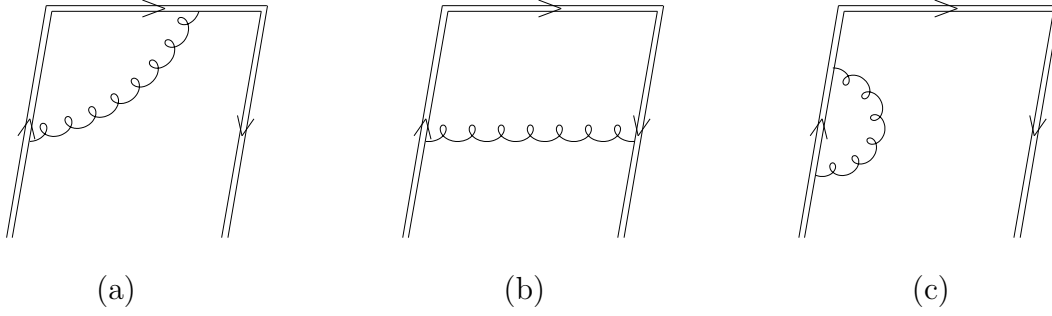


Figure 4: One-loop diagrams contributing to  $W(C_S)$ . Here, the double line represents the integration path in the Minkowski space as in fig. 2. The Feynman rules for these diagrams are given in the Appendix.

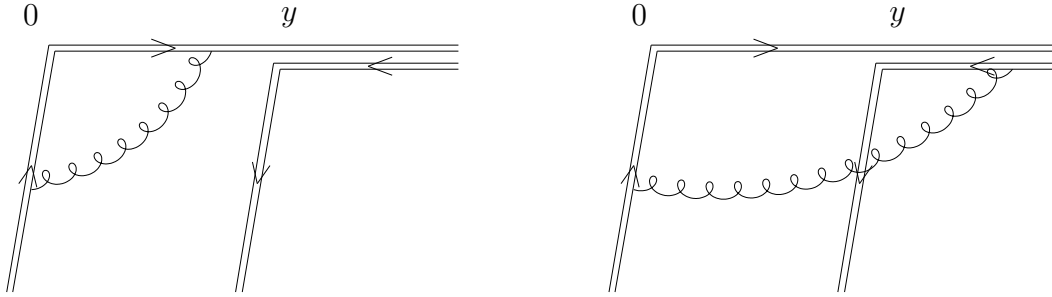


Figure 5: Diagrams corresponding to fig. 4a for virtual and real gluon (see (2.15)). Due to a partial cancellation of Wilson lines, the sum of these two diagram gives the single contribution of fig. 4a. Similar cancellations hold for all diagrams.

where  $C_F$  is the quadratic Casimir operator in the quark representation. For  $y_-$  positive the vector  $z = (z_2 - z_1)$  is time-like ( $z^2 > 0$  and  $z_0 > 0$ ) so that cutted and full propagators coincide:  $D_+^{\mu\nu}(z) = D^{\mu\nu}(z) = -g^{\mu\nu}D(z)$ . Then, the sum of the two diagrams of fig. 5 is

$$W_a^{(1)} = g^2 C_F (vy) \int_{-\infty}^0 dt_1 \int_0^1 dt_2 D(yt_2 - nt_1) \quad (2.16)$$

The same result is obtained for  $y_-$  negative by deforming the integration path  $\ell_1$ . To show this observe first that the singularities of the integrand in the  $t_1$ -complex plane lie in the lower half plane. Therefore we can deform the integration path from  $-\infty < t_1 < 0$  to  $0 < t_1 < \infty$ . After this deformation the vector  $yt_2 - vt_1$  becomes time-like and we have the same situation as for  $y_-$  positive.

Both the real and virtual contributions in (2.15) have infrared (IR) and UV singularities. The real and virtual IR singularities, coming from  $t_2 \rightarrow \infty$ , cancel in (2.16), giving a bonded range for  $t_2$ . This cancellation between the two paths from point  $y$  to  $\infty$  is general since it is the result of causality of Wilson lines in (2.10). For this reason in fig. 4 we neglect these parts of the integration paths.

Integral in eq.(2.16) is ultraviolet divergent and we use dimensional regularization. Using the  $D$ -dimensional propagator given in the Appendix we obtain

$$W_a^{(1)} = \frac{g^2}{4\pi^{D/2}} \mu^{4-D} \Gamma(D/2 - 1) C_F (vy) \int_{-\infty}^0 dt_1 \int_0^1 dt_2 (-t_1^2 + 2(vy)t_1 t_2 + i0)^{1-D/2}$$

which is divergent for  $D = 4$ . To see the origin of these divergences we change the integration variable to  $t_1 = -2(vy)t_2t'_1$  and obtain

$$W_a^{(1)} = -\frac{g^2}{8\pi^{D/2}}C_F\Gamma(D/2 - 1)[2i\mu(v \cdot y - i0)]^{4-D} \int_0^\infty dt'_1(t'_1(1 + t'_1))^{1-D/2} \int_0^1 dt_2 t_2^{3-D}$$

For  $D \rightarrow 4$  we find two singularities: for  $t_2 \rightarrow 0$  and  $t'_1 \rightarrow 0$ . In the first case we have  $z_2 - z_1 \rightarrow 0$ , which corresponds to the integration near the cusp at point 0. This singularity is called ‘‘cusp singularity’’ [13]. For  $t'_1 \rightarrow 0$  we have  $z_1 \rightarrow 0$  and  $(z_2 - z_1)^2 \rightarrow z_2^2 = 0$  which corresponds to the light-cone (collinear) singularity. The final unrenormalized result for this diagram is

$$W_a^{(1)} = -\frac{g^2}{4\pi^{D/2}}C_F[2i\mu(v \cdot y - i0)]^{4-D} \frac{\Gamma(3 - D/2)\Gamma(D - 3)}{(4 - D)^2} \quad (2.17)$$

For the diagram of fig. 4b we obtain

$$\begin{aligned} W_b^{(1)} &= (ig)^2 C_F \int_{-\infty}^0 dt_1 \int_0^\infty dt_2 D_+(y - v(t_2 + t_1)) \\ &= -\frac{g^2}{4\pi^{D/2}} \mu^{4-D} \Gamma(D/2 - 1) C_F \int_{-\infty}^0 dt_1 \int_0^\infty dt_2 \\ &\quad \times [2(y_- - v_-(t_2 + t_1) - i0)(v_+(t_2 + t_1) + i0)]^{1-D/2} \end{aligned}$$

This integral for  $D \rightarrow 4$  has an infrared singularity for  $z_2 - z_1 \rightarrow \infty$ . Taking  $D > 4$  one gets

$$W_b^{(1)} = \frac{g^2}{4\pi^{D/2}} C_F [2i\mu(v \cdot y - i0)]^{4-D} \frac{\Gamma(3 - D/2)\Gamma(D - 3)}{4 - D} \quad (2.18)$$

For the diagram of fig. 4c we have

$$\begin{aligned} W_c^{(1)} &= \frac{g^2}{4\pi^{D/2}} \mu^{4-D} \Gamma(D/2 - 1) C_F \int_{-\infty}^0 dt_1 \int_{t_1}^0 dt_2 (-(t_1 - t_2)^2 + i0)^{1-D/2} \\ &= -\frac{g^2}{4\pi^{D/2}} C_F (\mu^2 v^2)^{2-D/2} i^{4-D} \frac{\Gamma(D/2 - 1)}{3 - D} \int_{-\infty}^0 dt_1 t_1^{3-D}. \end{aligned} \quad (2.19)$$

In this case we have an IR singularity for  $D < 4$  as  $t_1 - t_2 \rightarrow \infty$  and an UV divergence for  $D > 4$  as  $t_1 \rightarrow 0$  and  $t_1 - t_2 \rightarrow 0$ . The IR divergence of  $W_c^{(1)}$  is cancelled by the IR divergence of  $W_b^{(1)}$ . Thus, the sum of the diagrams  $W_b^{(1)} + W_c^{(1)}$  contains only UV divergence. This IR cancellation does not depend on the scheme we use to regularize IR divergences, *e.g.* by putting a cutoff in the  $t_i$ -integration or by giving a fictitious mass to the gluon.

Notice, that the IR and UV poles in  $W_c^{(1)}$  have opposite coefficients, thus one can formally set  $W_c^{(1)} = 0$ . In this case however the pole of  $W_b^{(1)}$  for  $D = 4$  has to be interpreted as an UV singularity.

Summing eqs.(2.17), (2.18) and the symmetric contributions we obtain the one-loop expression for the unrenormalized Wilson loop (2.13)

$$W^{(1)} = \frac{g^2}{4\pi^{D/2}} C_F [2i\mu(v \cdot y - i0)]^{4-D} \Gamma(3 - D/2)\Gamma(D - 3) \left( -\frac{2}{(4 - D)^2} + \frac{1}{4 - D} \right). \quad (2.20)$$

By subtracting the poles in the  $\overline{\text{MS}}$ -scheme we obtain

$$W_{ren.}^{(1)} = \frac{\alpha_s}{\pi} C_F \left( -L^2 + L - \frac{5}{24} \pi^2 \right), \quad L = \ln(i(\rho - i0)) + \gamma_E \quad (2.21)$$

where

$$\rho = (vy)\mu = (Py) \frac{\mu}{M}, \quad y = (0, \mathbf{0}, y_-). \quad (2.22)$$

From eqs.(2.20) and (2.21) we can directly see that  $W(C_S)$  to one loop depends only on the variable  $\rho$  and the possible singularities are in the upper half plane

$$W(C_S) = W(\rho - i0). \quad (2.23)$$

This is due to the fact that  $\rho$  is the only scalar dimensionless variable formed by  $v$ ,  $y$  and  $\mu$ . The “ $-i0$ ” prescription comes from the position of the pole in the free gluon propagator in the coordinate representation. Moreover, expression (2.21) implies that under complex conjugation

$$W(\rho - i0) = (W(-\rho - i0))^* .$$

It is this property that ensures the reality condition of the distribution function (2.12).

### 3. Two-loop calculation

In this section we perform the two-loop calculation of  $W(C_S)$ . In order to simplify the calculation and reduce the number of diagrams to compute we use the nonabelian exponentiation theorem [14]. According to this theorem we can write

$$W \equiv 1 + \sum_{n=1}^{\infty} \left( \frac{\alpha_s}{\pi} \right)^n W^{(n)} = \exp \sum_{n=1}^{\infty} \left( \frac{\alpha_s}{\pi} \right)^n w^{(n)}$$

where  $w^{(n)}$  is given by the contributions of  $W^{(n)}$  with the “maximal nonabelian color and fermion factors” to the  $n$ -th order of perturbation theory. At one loop we have only the color factor  $C_F$ . At two-loops the maximal nonabelian color factor is  $C_A C_F$  and the fermionic factor is  $C_F N_f$ . Here,  $C_A$  is the quadratic Casimir operator in the gluon representation and  $N_f$  the number of light quarks. From this theorem we have  $W^{(1)} = w^{(1)}$  and

$$W^{(2)} = \frac{1}{2}(w^{(1)})^2 + w^{(2)}$$

and the contributions with the abelian color factor  $C_F^2$  are contained only in the first term.

In fig. 6 we list all nonvanishing the two-loop diagrams which contain color factors  $C_F C_A$  and  $C_F N_f$ . As for the one loop case, the paths in these diagrams do not contain the two rays from  $y$  to  $\infty$  because their contributions cancel due to causality of Wilson lines in (2.10).

The color factor of abelian-like diagrams of figs. 6.1-6.6 is  $C_F(C_F - \frac{1}{2}C_A)$ . These diagrams contribute to  $w^{(2)}$  with the color factor  $-\frac{1}{2}C_F C_A$ . Diagrams with gluon self-energy of figs. 6.7 and 6.8 will contain contributions with both color factors  $C_F C_A$  and  $C_F N_f$ . The latter one comes from the quark loop contribution. Finally, diagrams of figs. 6.9-6.11 are of nonabelian nature involving three-gluon coupling and their color factor is proportional to  $C_F C_A$ . We have omitted diagrams with abelian color factor  $C_F^2$ , diagrams vanishing due to the antisymmetry of three-gluon vertex,

diagrams proportional to  $y^2 = 0$  and self-energy like diagrams obtained by iterating the one-loop diagram in fig. 4c. The reason for neglecting of the latter type of diagrams is the following. As in the one-loop case the self-energy diagrams have both IR and UV poles which cancel each other. On the other hand in the sum of all two loop diagrams the IR singularities cancel completely. Therefore, as we did for one-loop case, we neglect the self-energy diagrams and interpret the IR poles in the diagrams of fig. 6 as UV singularities.

For the diagrams of figs. 6.2–6.5 and figs. 6.8 and 6.10 we have to consider contributions involving cutted propagators. As we have observed before, there is no difference between real and virtual gluon propagating in the time-like direction ( $D(z) = D_+(z)$  for time-like  $z$ ). This gives rise to a partial cancellation between real and virtual contributions. This cancellation has been already used to simplify the analysis in the one-loop case (2.19) and we will further exploit it in this section. It turns out that to compute singular contributions for  $D = 4$  we can replace the cutted propagators in fig. 6 by full ones. This is due to the fact that one can always deform the integration path in such a way that gluons propagate in the time-like direction.

### 3.1. Abelian like diagrams

The general form of the contribution of the abelian like diagrams of figs. 6.1–6.6 is ( $a = 1, \dots, 6$ )

$$W_a = \left( \frac{g^2}{4\pi^{D/2}} \right)^2 C_F (C_F - \frac{1}{2}C_A) [2i(\rho - i0)]^{8-2D} I_a(D) \quad (3.1)$$

where  $I_a(D)$  is a function of  $D$  and the index  $a$  refers to the diagrams in fig. 6 and  $\rho$  is given in (2.23).

Diagram of fig. 6.1 gives

$$W_1 = g^4 C_F (C_F - \frac{1}{2}C_A) (vy) \int_{-\infty}^0 dt_1 \int_{t_1}^0 dt_2 \int_{t_2}^0 dt_3 \int_0^1 dt_4 D(z_3 - z_1) D(z_4 - z_2)$$

with

$$D(z_3 - z_1) D(z_4 - z_2) = \left( \frac{\Gamma(D/2 - 1)}{4\pi^{D/2}} \right)^2 \left[ (t_1 - t_3)^2 t_2 \left( t_2 - \frac{y_-}{v_-} t_4 \right) \right]^{1-D/2}$$

where  $z_i = vt_i$ ,  $i = 1, 2, 3$  and  $z_4 = yt_4$ . This diagram contain UV divergence for  $z_1 - z_3 \rightarrow 0$  corresponding to vertex renormalization. The rest of the diagram has the same divergences as one loop diagram of fig. 4a. Namely, it has a cusp singularity for  $z_4 - z_2 \rightarrow 0$  and light-cone collinear singularity for  $z_2 \rightarrow 0$ . Performing the integration we obtain

$$I_1 = - \frac{\Gamma(D/2 - 1) \Gamma(7 - 3D/2) \Gamma(2D - 7)}{6(3 - D)(4 - D)^3}$$

Diagram of fig. 6.2 gives

$$W_2 = -g^4 C_F (C_F - \frac{1}{2}C_A) \int_{-\infty}^0 dt_1 \int_{t_1}^0 dt_2 \int_{t_2}^0 dt_3 \int_0^\infty dt_4 D(z_3 - z_1) D_+(z_4 - z_2)$$

with

$$D(z_3 - z_1) D_+(z_4 - z_2) = \left( \frac{\Gamma(D/2 - 1)}{4\pi^{D/2}} \right)^2 \left[ (t_1 - t_3)^2 (t_2 + t_4 + i0) \left( t_2 + t_4 - \frac{y_-}{v_-} + i0 \right) \right]^{1-D/2}$$

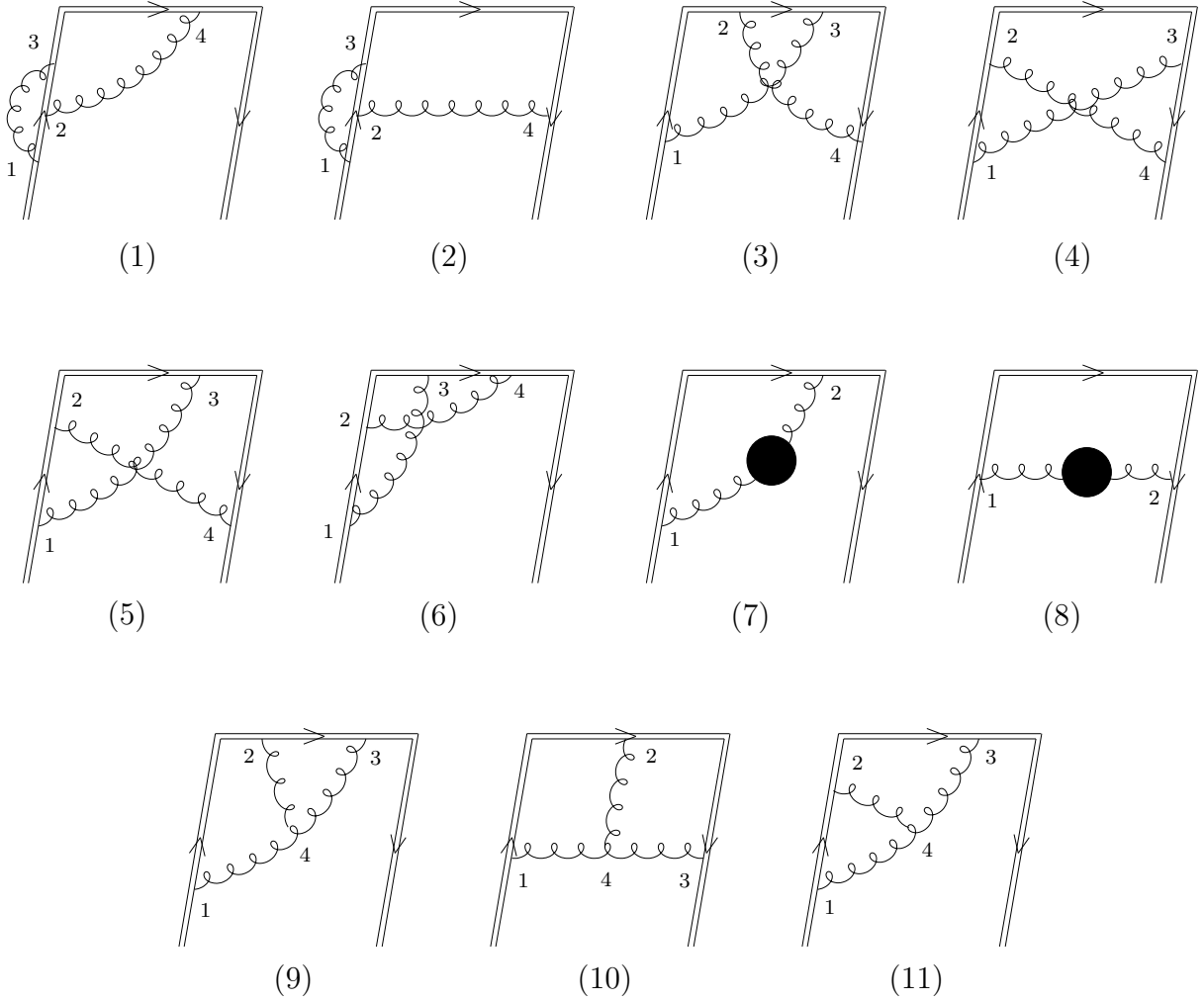


Figure 6: Nonvanishing two-loop diagrams containing the “maximally nonabelian” color  $C_A C_F$  and the fermionic  $C_F N_f$  factors. Due to the exponentiation theorem, these are the only diagram we need to evaluate to compute the two-loop contribution of  $W(C_S)$ . The blob denotes the sum of gluon, quark and ghost loops.

where  $z_i = vt_i$ ,  $i = 1, 2, 3$  and  $z_4 = y - vt_4$ . The analysis of singularities is similar to the previous case. We have a UV singularity for  $z_1 - z_3 \rightarrow 0$  and a IR pole originated from one-loop diagram of fig. 4b. The result of the integration is

$$I_2 = \frac{\Gamma(D/2 - 1)\Gamma(7 - 3D/2)\Gamma(2D - 7)}{2(3 - D)(4 - D)^2(5 - D)}$$

Diagram of fig. 6.3 gives

$$W_3 = -g^4 C_F (C_F - \frac{1}{2} C_A) (vy)^2 \int_{-\infty}^0 dt_1 \int_0^1 dt_2 \int_{t_2}^1 dt_3 \int_0^\infty dt_4 D(z_3 - z_1) D_+(z_4 - z_2),$$

where  $z_1 = vt_1$ ,  $z_2 = yt_2$ ,  $z_3 = yt_3$  and  $z_4 = y - vt_4$ . Since all singularity in  $t_4$ -plane lie at the lower half-plane we deform the  $t_4$ -integration path from  $[0, \infty)$  to  $(-\infty, 0]$ . After this transformation  $z_4$  is replaced by  $z'_4 = y + vt_4$  and  $z'_4 - z_2$  becomes time-like vector for which cutted and full

propagators are the same. We can than replace

$$D(z_3 - z_1)D_+(z_4 - z_2) \Rightarrow D(z_3 - z_1)D_+(z'_4 - z_2) = D(z_3 - z_1)D(z'_4 - z_2)$$

which gives

$$D(z_3 - z_1)D(z'_4 - z_2) = \left( \frac{\Gamma(D/2 - 1)}{4\pi^{D/2}} \right)^2 \left[ t_1 t_2 \left( t_1 - \frac{y_-}{v_-} t_3 \right) \left( t_4 + \frac{y_-}{v_-} (1 - t_2) \right) \right]^{1-D/2}.$$

This diagram has two light-cone collinear singularities for  $z_1 \rightarrow 0$  and  $z_4 \rightarrow y$ . Evaluating the integral we obtain

$$I_3 = \frac{\Gamma^2(3 - D/2)\Gamma^2(D - 3)}{(4 - D)^4} \left( 1 - \frac{\Gamma^2(5 - D)}{\Gamma(9 - 2D)} \right).$$

The diagram of fig. 6.4 gives

$$W_4 = g^4 C_F (C_F - \frac{1}{2} C_A) \int_{-\infty}^0 dt_1 \int_{t_1}^0 dt_2 \int_0^\infty dt_3 \int_{t_3}^\infty dt_4 D_+(z_3 - z_1) D_+(z_4 - z_2)$$

where  $z_i = vt_i$  for  $i = 1, 2$  and  $z_j = y - vt_j$  for  $j = 3, 4$ . As in the previous diagram we can deform  $z_3$  and  $z_4$  integration paths by replacing  $z_j = y - vt_j$  with  $z'_j = y + vt_j$  for  $j = 3, 4$  corresponding to the replacement

$$D_+(z_3 - z_1)D_+(z_4 - z_2) \Rightarrow D_+(z'_3 - z_1)D_+(z'_4 - z_2) = D(z'_3 - z_1)D(z'_4 - z_2)$$

and we have

$$D(z'_3 - z_1)D(z'_4 - z_2) = \left( \frac{\Gamma(D/2 - 1)}{4\pi^{D/2}} \right)^2 \left[ (t_4 - t_2 + \frac{y_-}{v_-})(t_4 - t_2)(t_3 - t_1 + \frac{y_-}{v_-})(t_3 - t_1) \right]^{1-D/2}.$$

This diagram has a single IR pole for  $z_4 - z_2 \rightarrow \infty$  and  $z_3 - z_1 \rightarrow \infty$  simultaneously. Evaluating the integral we obtain

$$I_4 = -\frac{1}{4 - D} \frac{\Gamma(2D - 7)}{2\Gamma^2(D/2 - 1)} + \mathcal{O}((4 - D)^0).$$

Diagram of fig. 6.5 gives

$$W_5 = -g^4 C_F (C_F - \frac{1}{2} C_A) \int_{-\infty}^0 dt_1 \int_{t_1}^0 dt_2 \int_0^1 dt_3 \int_0^\infty dt_4 D(z_3 - z_1) D_+(z_4 - z_2),$$

where  $z_i = vt_i$  for  $i = 1, 2$ ,  $z_3 = yt_3$  and  $z_4 = y - vt_4$ . Deforming the  $z_4$  integration path we replace  $z_4$  with  $z'_4 = y + vt_4$

$$D(z_3 - z_1)D_+(z_4 - z_2) \Rightarrow D(z_3 - z_1)D_+(z'_4 - z_2) = D(z_3 - z_1)D(z'_4 - z_2)$$

and we have

$$D(z_3 - z_1)D(z'_4 - z_2) = \left( \frac{\Gamma(D/2 - 1)}{4\pi^{D/2}} \right)^2 \left[ t_1 \left( t_1 - \frac{y_-}{v_-} t_3 \right) \left( t_4 - t_2 + \frac{y_-}{v_-} \right) (t_4 - t_2) \right]^{1-D/2}.$$

It turns out that this diagram has no singularities for  $D = 4$ . To confirm this we evaluate the integral and obtain

$$I_5 = -\Gamma^2(D/2 - 1) \left\{ -\frac{\pi^2}{3} + \frac{1}{(4-D)^3(3-D)} \left( \frac{3\Gamma(3-D/2)\Gamma(2D-7)}{\Gamma(3D/2-5)} - \frac{\Gamma(5-D)\Gamma(2D-7)}{\Gamma(D-3)} - \frac{2\Gamma(3-D/2)\Gamma(D-3)}{\Gamma(D/2-1)} \right) \right\} = \mathcal{O}((4-D)^0).$$

Diagram of fig. 6.6 gives

$$W_6 = g^4 C_F (C_F - \frac{1}{2} C_A) (vy)^2 \int_{-\infty}^0 dt_1 \int_{t_1}^0 dt_2 \int_0^1 dt_3 \int_{t_3}^1 dt_4 D(z_3 - z_1) D(z_4 - z_2)$$

where  $z_i = vt_i$  for  $i = 1, 2$ ,  $z_j = yt_j$  for  $j = 3, 4$ , and we have

$$D(z_3 - z_1) D(z_4 - z_2) = \left( \frac{\Gamma(D/2 - 1)}{4\pi^{D/2}} \right)^2 \left[ t_1 t_2 \left( \frac{y_-}{v_-} t_3 - t_1 \right) \left( \frac{y_-}{v_-} t_4 - t_2 \right) \right]^{1-D/2}.$$

This diagram has two cusps singularities for  $z_3 - z_1 \rightarrow 0$  and  $z_4 - z_2 \rightarrow 0$  and two light-cone collinear singularities for  $z_1 \rightarrow 0$  and  $z_2 \rightarrow 0$ . Evaluating the integral we obtain

$$I_6 = \Gamma^2(D/2 - 1) \left\{ \frac{1}{(4-D)^4} \left( \frac{\Gamma(5-D)\Gamma(2D-7)}{2\Gamma(D-3)} - \frac{\Gamma(7-3D/2)\Gamma(2D-7)}{3\Gamma(D/2-1)} - \frac{1}{4} (2-D)(3-D/2)\Gamma(D-3) \left( \Gamma(5-D) - \frac{\Gamma(3-D/2)}{\Gamma(D/2-1)} \right) \right) - \frac{1}{4-D} \frac{\zeta(3)}{2} \right\} + \mathcal{O}((4-D)^0),$$

where  $\zeta(3)$  is the Reimann function.

### 3.2. Self-energy diagrams

The general form of the contribution of the diagrams with gluon self-energy in figs. 6.7 and 6.8 is ( $a = 7, 8$ )

$$W_a = \left( \frac{g^2}{4\pi^{D/2}} \right)^2 C_F ((3D-2)C_A - 2(D-2)N_f) [2i(\rho - i0)]^{8-2D} I_a(D).$$

The one-loop correction to the gluon propagator in the Feynman gauge in the coordinate representation is given by

$$D^{(1)}(z) = \frac{g^2}{64\pi^D} ((3D-2)C_A - 2(D-2)N_f) \frac{\Gamma^2(D/2-1)}{(D-4)(D-3)(D-1)} (-z^2 + i0)^{3-D} \quad (3.2)$$

which differs from the free propagator in the power of  $z^2 - i0$ . For time-like vector  $z$  the cutted one-loop propagator coincides with the full propagator in (3.2). As in the one loop case this allows us to treat the sum of these diagrams with all possible cuts by using the full propagator. We obtain

$$W_7 = g^2 C_F (vy) \int_{-\infty}^0 dt_1 \int_0^1 dt_2 D^{(1)}(z_2 - z_1)$$



where  $z_1 = vt_1$  and  $z_2 = yt_2$  and

$$W_8 = -g^2 C_F(vy) \int_{-\infty}^0 dt_1 \int_0^{\infty} dt_2 D_+^{(1)}(z_2 - z_1)$$

where  $z_1 = vt_1$  and  $z_2 = y - vt_2$ . By performing the integration we get

$$I_7 = \frac{\Gamma^2(D/2 - 1)\Gamma(5 - D)\Gamma(2D - 7)}{16(4 - D)^3(1 - D)\Gamma(D - 2)}, \quad I_8 = -\frac{\Gamma^2(D/2 - 1)\Gamma(5 - D)\Gamma(2D - 7)}{8(4 - D)^2(1 - D)\Gamma(D - 2)}$$

### 3.3. Diagrams with three-gluon vertices

For the diagrams of figs. 6.9–6.11 containing three-gluon vertex we have the following general expression

$$W_a = \frac{1}{2} C_A C_F \left( \frac{g^2}{4\pi^{D/2}} \right)^2 [2i(\rho - i0)]^{8-2D} I_a(D)$$

where  $a$  refers to the various diagrams in fig. 6 with three-gluon vertex. We simplify the analysis of the diagrams with various cuts by computing only the contributions which are singular for  $D \rightarrow 4$ . In this case we can treat all gluons as virtual. To show this observe that for the cutted diagrams at  $D = 4$  we have only infrared and light-cone collinear singularities. The infrared singularities cancel. The collinear singularities appear when gluons propagate along the light-cone, *i.e.* when the intermediate point  $z_4$  lies on the segment  $[0, y]$ . In this case cutted propagators coincide with the full propagators. Notice that cusp singularities appear when all gluons interact at small distances. They are present only for diagrams of figs. 6.9 and 6.11 for  $z_i \rightarrow 0$ . In this case all gluons are virtual. Therefore, in the following we study only the contributions to  $W_a$  in which all gluons are virtual.

For the diagram of fig.6.9 we have

$$W_9 = \frac{1}{2} g^4 C_A C_F \int_{-\infty}^0 dt_1 \int_0^1 dt_2 \int_{t_2}^1 dt_3 \int d^D z_4 v^{\mu_1} y^{\mu_2} y^{\mu_3} \Gamma_{\mu_1 \mu_2 \mu_3}(z_1, z_2, z_3) \prod_{i=1}^3 D(z_i - z_4)$$

where  $z_1 = vt_1$ ,  $z_2 = yt_2$  and  $z_3 = yt_3$ . By using the expression for the three-gluon vertex in the Appendix A we find

$$v^{\mu_1} y^{\mu_2} y^{\mu_3} \Gamma_{\mu_1 \mu_2 \mu_3}(z_1, z_2, z_3) = i(vy) \left( y \frac{\partial}{\partial z_2} - y \frac{\partial}{\partial z_3} \right) = i(vy) \left( \frac{\partial}{\partial t_2} - \frac{\partial}{\partial t_3} \right). \quad (3.3)$$

Due to this particularly simple form of the three-gluon vertex the integration over  $t_2$  or  $t_3$  becomes trivial. For the first term the integration over  $t_2$  gives the contributions from the end points  $z_2 = 0$  and  $z_2 = z_3$ . For the second term the integration over  $t_3$  gives the contributions from  $z_3 = z_2$  and  $z_3 = 1$ . In all contributions, the integral over the intermediate point  $z_4$  is factorized into the following expression

$$\begin{aligned} J(z_1, z_2, z_3) &= \int d^D z_4 \prod_{i=1}^3 D(z_i - z_4) \\ &= \frac{i^{1-2D}}{32\pi^D} \frac{\Gamma(D-3)}{4-D} \int_0^1 ds (s(1-s))^{D/2-2} ((-z_1 + sz_2 + (1-s)z_3)^2 - i0)^{3-D} \end{aligned} \quad (3.4)$$

valid for  $z_2$  and  $z_3$  on the light-cone ( $z_2^2 = z_3^2 = (z_2 - z_3)^2 = 0$ ). The pole at  $D = 4$  corresponds to a light-cone singularity as  $z_4$  approaches the segment  $[0, y]$ . The meaning of the integral over the parameter  $s$  is the following. For  $D = 4$  one integrates over the free gluon propagator between the points  $z_1$  and  $z = sz_2 + (1 - s)z_3$ . Since the  $z$  lies on the light-cone between  $z_2$  and  $z_3$  the vector  $z - z_1$  is time-like. This confirms the expectation expressed at the beginning of this subsection that all collinear gluons propagate in the time-like direction.

Performing the remaining integration we obtain

$$I_9 = -\frac{\Gamma(5 - D)\Gamma(2D - 7)}{4(4 - D)^3} \left( \frac{\Gamma^2(D/2 - 1)}{(4 - D)\Gamma(D - 3)} - \frac{4\Gamma(7 - 3D/2)\Gamma(D/2 - 1)}{3(4 - D)\Gamma(5 - D)} + \frac{\Gamma^2(D/2 - 1)}{\Gamma(D - 2)} \right).$$

For the diagram of fig. 6.10 one deforms the integration path over  $z_3 = y - vt_3$  into  $z_3 = y + vt_3$ , replaces cutted propagators by full ones and obtains

$$W_{10} = \frac{1}{2}g^4 C_A C_F \int_{-\infty}^0 dt_1 \int_0^1 dt_2 \int_0^\infty dt_3 \int d^D z_4 v^{\mu_1} y^{\mu_2} n^{\mu_3} \Gamma_{\mu_1 \mu_2 \mu_3}(z_1, z_2, z_3) \prod_{i=1}^3 D(z_i - z_4),$$

where  $z_1 = vt_1$ ,  $z_2 = yt_2$  and  $z_3 = y + vt_3$ . By using the three-gluon vertex we find

$$\begin{aligned} v^{\mu_1} y^{\mu_2} n^{\mu_3} \Gamma_{\mu_1 \mu_2 \mu_3}(z_1, z_2, z_3) &= i \left( y \frac{\partial}{\partial z_1} - y \frac{\partial}{\partial z_3} \right) - i(vy) \left( v \frac{\partial}{\partial z_1} - v \frac{\partial}{\partial z_3} \right) \\ &= i \left( y \frac{\partial}{\partial z_1} - y \frac{\partial}{\partial z_3} \right) - i(vy) \left( \frac{\partial}{\partial t_1} - \frac{\partial}{\partial t_3} \right). \end{aligned}$$

The first term leads to a contribution which is regular for  $D = 4$ . To see this notice that the singularities arise when the gluons are propagating along the light-like vector  $y$ . However, this configuration is suppressed by applying the operator  $y \frac{\partial}{\partial z_i}$  to the gluon propagator. The expression  $y \frac{\partial}{\partial z_i} D(z_i - z_4)$  is proportional to  $y(z_i - z_4)$  and vanishes for  $z_i - z_4$  parallel to  $y$ . The second term is similar to the one of the previous diagram. We have contributions from the end-points  $z_1 = 0$  and  $z_3 = y$ . For  $z_1 = 0$  ( $z_3 = y$ ) the two vectors  $z_1$  and  $z_2$  ( $z_2$  and  $z_3$ ) lie on the light-cone and we can apply the identity (3.4). Performing the remaining integrations we obtain

$$I_{10} = -\frac{\Gamma(5 - D)\Gamma(2D - 7)\Gamma(D/2 - 1)}{2(4 - D)^4} \left( \frac{\Gamma(D/2 - 1)}{\Gamma(D - 3)} - \frac{\Gamma(7 - 3D/2)}{\Gamma(5 - D)} \right).$$

For the last diagram of fig. 6.11 we have

$$W_{11} = \frac{1}{2}g^4 C_A C_F \int_{-\infty}^0 dt_1 \int_{t_1}^0 dt_2 \int_0^\infty dt_3 \int d^D z_4 v^{\mu_1} v^{\mu_2} y^{\mu_3} \Gamma_{\mu_1 \mu_2 \mu_3}(z_1, z_2, z_3) \prod_{i=1}^3 D(z_i - z_4),$$

where  $z_1 = vt_1$ ,  $z_2 = vt_2$  and  $z_3 = yt_3$ . By using three-gluon vertex we obtain

$$\begin{aligned} v^{\mu_1} v^{\mu_2} y^{\mu_3} \Gamma_{\mu_1 \mu_2 \mu_3}(z_1, z_2, z_3) &= -i \left( y \frac{\partial}{\partial z_1} - y \frac{\partial}{\partial z_2} \right) + i(vy) \left( v \frac{\partial}{\partial z_1} - v \frac{\partial}{\partial z_2} \right) \\ &= -i \left( y \frac{\partial}{\partial z_1} - y \frac{\partial}{\partial z_2} \right) + i(vy) \left( \frac{\partial}{\partial t_1} - \frac{\partial}{\partial t_2} \right). \end{aligned} \quad (3.5)$$

For this diagram we have the following singularities: a cusp singularity for  $z_i \rightarrow 0$  with  $i = 1, \dots, 4$ ; two independent light-cone collinear singularities for  $z_1, z_2 \rightarrow 0$  and  $z_4$  approaching the segment  $[0, y]$ ; an ultraviolet singularity from  $z_2, z_4 \rightarrow z_1$ .

The operator  $y \frac{\partial}{\partial z_i}$  in the first term suppresses propagation along light-like vector  $y$  of gluon from point  $z_4$  to  $z_1$  or to  $z_2$ . This implies that the contribution of this part of three-gluon vertex contains only a triple pole in  $4 - D$ . The second term in (3.5) is similar to the one in (3.3) for diagram of fig. 6.9. We have two end-point contributions with  $z_2 = 0$  and  $z_1 = z_2$ . For  $z_2 = 0$  the two vectors  $z_2$  and  $z_3$  lie on the light-cone and we can apply the identity (3.4). For  $z_1 = z_2$  the integral is similar to the one of the gluon self-energy correction.

We finally obtain

$$I_{11} = \frac{\Gamma(5 - D)\Gamma(2D - 6)}{4(4 - D)} \left( \frac{\Gamma(3D/2 - 5)\Gamma(3 - D/2)}{3\Gamma(D - 2)(4 - D)^3} - \frac{1}{2} \zeta(3) \right). \quad (3.6)$$

Recall that all expressions in this subsection are valid up to terms which are regular for  $D = 4$ .

### 3.4. Renormalization at two-loop order

Since the diagrams of fig. 6 have nested ultraviolet divergences corresponding to the renormalization of the vertices and propagators one has to include additional counter-terms. In the  $\overline{\text{MS}}$ -scheme their contributions are given to two loops by

$$w_{c.t.}^{(2)} = \left( \frac{\alpha_s}{\pi} \right)^2 C_F \left( \frac{11}{3} C_A - \frac{2}{3} N_f \right) [2i(\rho - i0)]^{4-D} \frac{\Gamma(3 - D/2)\Gamma(D - 3)}{(4 - D)^2} \left( \frac{1}{4 - D} - \frac{1}{2} \right).$$

To obtain the final expression for the renormalized  $w$  to two-loops we add the counter-terms, subtract the poles in the  $\overline{\text{MS}}$ -scheme and take into account combinatorial factors. By using the non-abelian exponentiation theorem  $w^{(2)}$  is obtained by omitting the colour factor  $C_F^2$  in (3.1). The final contributions to  $w^{(2)}$  from the various diagrams ( $a = 1, \dots, 11$ ) have the following form

$$w_a^{(2)} = \left( \frac{\alpha_s}{\pi} \right)^2 C_F [C_A(A_a L^4 + B_a L^3 + C_a L^2 + D_a L) + N_f(E_a L^3 + F_a L^2 + G_a L) + \mathcal{O}(L^0)]$$

where  $L$  is given in (2.21) and for the various diagrams the nonvanishing coefficients are given by

$$\begin{aligned} A_6 &= -\frac{1}{9}, & A_9 &= \frac{1}{18}, & A_{11} &= \frac{1}{18}, \\ B_1 &= -\frac{2}{9}, & B_7 &= -\frac{5}{9}, & B_9 &= -\frac{1}{3}, & B_{11} &= -\frac{1}{9}, & B_{c.t.} &= \frac{11}{18}, \\ C_1 &= -\frac{1}{3}, & C_2 &= 1, & C_3 &= -\frac{\pi^2}{6}, & C_6 &= -\frac{7}{72}\pi^2, & C_7 &= -\frac{31}{36}, \\ C_8 &= \frac{5}{6}, & C_9 &= \frac{25}{144}\pi^2 - \frac{1}{2}, & C_{10} &= \frac{1}{12}\pi^2, & C_{11} &= \frac{13}{144}\pi^2 - \frac{1}{6}, & C_{c.t.} &= -\frac{11}{12}, \\ D_1 &= -\frac{13}{72}\pi^2 - \frac{1}{3}, & D_3 &= 2\zeta(3), & D_4 &= \frac{1}{2}, & D_6 &= \frac{2}{9}\zeta(3), & D_7 &= -\frac{47}{54} - \frac{5}{16}\pi^2, & D_8 &= \frac{31}{36}, \\ D_9 &= \frac{1}{72}\zeta(3) - \frac{1}{2} - \frac{3}{16}\pi^2, & D_{10} &= -\frac{1}{4}\zeta(3), & D_{11} &= -\frac{13}{144}\pi^2 + \frac{19}{72}\zeta(3) - \frac{1}{6}, & D_{c.t.} &= \frac{55}{144}\pi^2, \\ E_7 &= \frac{2}{9}, & E_{c.t.} &= -\frac{1}{9}, \\ F_7 &= \frac{5}{18}, & F_8 &= -\frac{1}{3}, & F_{c.t.} &= \frac{1}{6}, \\ G_7 &= \frac{1}{8}\pi^2 + \frac{7}{27}, & G_8 &= -\frac{5}{18}, & G_{c.t.} &= -\frac{5}{72}\pi^2. \end{aligned}$$

Summing all contributions we finally obtain

$$w^{(2)} = \left( \frac{\alpha_s}{\pi} \right)^2 C_F (BL^3 + CL^2 + DL + \mathcal{O}(L^0)) \quad (3.7)$$

where

$$\begin{aligned}
B &= -\frac{11}{18}C_A + \frac{1}{9}N_f, \\
C &= \left(\frac{1}{12}\pi^2 - \frac{17}{18}\right)C_A + \frac{1}{9}N_f, \\
D &= \left(\frac{9}{4}\zeta(3) - \frac{7}{18}\pi^2 - \frac{55}{108}\right)C_A + \left(\frac{1}{18}\pi^2 - \frac{1}{54}\right)N_f.
\end{aligned}$$

This expression has the following properties:

- the coefficient of  $L^4$  vanishes;
- the coefficient of  $L^3$  is proportional to the one-loop beta-function;
- the interpretation of the remaining coefficients in front of  $L^2$  and  $L$  will be clear from the RG equation for light-like Wilson loop we are going to discuss in sect. 4.

The two-loop calculation confirms the analytical dependence in (2.23) which means that all singularities of  $W(C_S)$  in the complex  $\rho$ -plane lie in the upper half plane. After integration over  $y_-$  in (2.12) this leads to the spectral property

$$F(x, \mu/M) = 0 \quad \text{for } x > 1. \quad (3.8)$$

It has been observed [15] that the presence in (3.7) of the  $L^3$  term seems to be in contradiction with the renormalization properties of Wilson loops. Assuming that  $W(C_S)$  is renormalized multiplicatively, the  $L^3$  term should vanish. However one should notice that we are dealing with a light-like Wilson loop which has additional light-cone singularities. Moreover, the fact that the coefficient of  $L^3$  is just the one-loop beta-function suggests that light-like Wilson loop obeys a RG equation. This equation is discussed in the next section.

## 4. Renormalization group equation for Wilson loop on the light-cone

To evaluate the structure function for  $x \rightarrow 1$  given in eq.(2.12) one needs to compute  $W(C_S)$  in (2.13) to all orders in perturbation theory. A powerful method to resum the expansion is the use of renormalization group equation. In this section, following ref. [16], we deduce the RG equation of Wilson loops with path partially lying on the light-cone.

Recall that for  $x$  away from 1 the operator product expansion on the light-cone allows us to relate the  $\mu$ -dependence of the structure function with the ultraviolet properties of local composite twist-2 operators obtained by expanding in powers of  $y_-$  the matrix element in (2.1). This dependence is described by the evolution equations [8]

$$\left(\mu \frac{\partial}{\partial \mu} + \beta(g) \frac{\partial}{\partial g}\right) F(x, \mu/M) = \int_x^1 dz P(x/z) F(z, \mu/M), \quad (4.1)$$

where the splitting function  $P(z)$  is singular for  $z \rightarrow 1$ . For  $x \rightarrow 1$  the structure function (2.12) is given in terms of  $W(C_S)$ , which is a nonlocal operator. This suggests that it is convenient to treat the Wilson loop as a nonlocal functional of gauge field rather than to expand it into sum of infinitely many local composite operators. This can be done by using RG equation of  $W(C_S)$ , which gives the dependence on the renormalization point  $\mu$ . Since  $W(C_S)$  is a function of the single parameter  $\rho \sim \mu y_-$ , from its  $\mu$  dependence we directly obtain the dependence on  $y_-$  and, through Fourier transform in (2.12), the dependence on  $x$  for the structure function.

## 4.1. Wilson loop renormalization away from the light-cone

Renormalization group equation for the Wilson loop away from the light-cone is well known [13] and depends on the explicit form of the path. The integration path for  $W(C_S)$  is shown in fig. 2. It has two cusps at the points 0 and  $y$  where the quark is probed by the photon. The important property of this path is that the segment  $\ell_2$  lies on the light-cone. As we discussed in the two loop calculation, the presence of the  $L^3$  term entails that the renormalization properties of  $W(C_S)$  are different from the ones of Wilson loops with path away from the light cone.

Suppose for a moment that  $\ell_2$  lies away from the light-cone, *i.e.*  $y^2 \neq 0$ . Then, the dependence on  $\mu$  of the renormalized Wilson loop expectation value is described by the RG equation

$$\left( \mu \frac{\partial}{\partial \mu} + \beta(g) \frac{\partial}{\partial g} \right) \ln W_{(y^2 \neq 0)}(C_S) = -\Gamma_{\text{cusp}}(\gamma_+, g) - \Gamma_{\text{cusp}}(\gamma_-, g), \quad (4.2)$$

where  $\gamma_{\pm}$  are the angles in Minkowski space between vectors  $\pm y_{\mu}$  and  $v_{\mu} = p_{\mu}/M$  with  $v^2 = 1$

$$\cosh \gamma_{\pm} = \pm \frac{(vy)}{\sqrt{y^2}}.$$

The cusp anomalous dimension  $\Gamma_{\text{cusp}}(\gamma, g)$  is gauge invariant function of the cusp angle [13]. In the limit of large angles  $\gamma$  we have [17]

$$\Gamma_{\text{cusp}}(\gamma, g) = \gamma \Gamma_{\text{cusp}}(g) + \mathcal{O}(\gamma^0),$$

where the coefficient  $\Gamma_{\text{cusp}}(g)$  is known to two loop order and is given by

$$\Gamma_{\text{cusp}}(g) = \frac{\alpha_s}{\pi} C_F + \left( \frac{\alpha_s}{\pi} \right)^2 C_F \left( C_A \left( \frac{67}{36} - \frac{\pi^2}{12} \right) - N_f \frac{5}{18} \right). \quad (4.3)$$

For the integration path of fig. 2 we have  $y^2 = 0$  leading to an infinite  $\gamma_{\pm}$ , thus eq.(4.2) becomes meaningless. One can directly check that the two-loop result of previous section does not satisfy equation (4.2). However, as shown in subsect. 4.2, there is a simple way to find the generalization of the renormalization group equation for the light-cone Wilson loop.

## 4.2. Wilson loop renormalization on the light-cone

Renormalization group equation for Wilson loops on the light-cone has been proposed in [16] and can be obtained as follows. First, one slightly shifts the integration path away from the light-cone by setting  $y^2 \neq 0$  and keeping the cusp angle  $\gamma_{\pm} = \frac{1}{2} \ln(4(vy)^2/y^2)$  large. Since  $\gamma_{\pm}$  is a logarithmic function of  $(vy)$  and  $y^2$  we need to define its analytical continuation away from positive  $(vy)$  and  $y^2$ . The proper expressions for  $\gamma_{\pm}$  can be deduced from one-loop calculation of Wilson loop [16] and are given by

$$\gamma_+ = \frac{1}{2} \ln \frac{4((vy) - i0)^2}{y^2 - i0}, \quad \gamma_- = \frac{1}{2} \ln \frac{4((vy) + i0)^2}{y^2 - i0}$$

where the “ $-i0$ ” prescription comes from the position of the singularity of the free gluon propagator in the coordinate representation. By using these expressions we now differentiate the

renormalization group equation (4.2) with respect to the variable  $(vy)$

$$\left(\mu \frac{\partial}{\partial \mu} + \beta(g) \frac{\partial}{\partial g}\right) \frac{\partial}{\partial (vy)} \ln W(C_S) = -\Gamma_{\text{cusp}}(g) \left(\frac{1}{(vy) - i0} + \left(\frac{1}{(vy) + i0}\right)^\dagger\right) = -\frac{2\Gamma_{\text{cusp}}(g)}{(vy) - i0}. \quad (4.4)$$

The two terms originate from two cusps of the path of fig. 2 which lie on the opposite sides of the cut. This is the reason for the appearance of complex conjugation in the second term.

The variable  $y^2$  disappeared from this equation and one can formally set  $y^2 = 0$ . This is the proposed renormalization group equation for the Wilson loop on the light-cone [16]. One easily check that two-loop expression (3.7) of the previous section does satisfy eq.(4.4).

Notice, that Wilson loop on the light-cone depends only on a single variable  $L = \ln(i(\rho - i0)) + \gamma_E$ . Thus equation (4.4) becomes very powerful since one can integrate it and obtain RG equation for the light-like Wilson loop

$$\left(\mu \frac{\partial}{\partial \mu} + \beta(g) \frac{\partial}{\partial g}\right) W(C_S) = -[2\Gamma_{\text{cusp}}(g)L + \Gamma(g)] W(C_S), \quad (4.5)$$

where  $\Gamma(g)$  is the integration constant. From this equation we can see the origin of the various terms in the two-loop calculations in (3.7). The appearance of the one-loop beta function in front of the  $L^3$  term is obvious from (4.5). The coefficient of  $L^2$  is proportional to a sum of  $\Gamma_{\text{cusp}}(g)$  and one-loop beta-function. The coefficient of  $L$  is given by

$$\Gamma(g) = -\frac{\alpha_s}{\pi} C_F + \left(\frac{\alpha_s}{\pi}\right)^2 C_F \left[\left(\frac{55}{108} + \frac{1}{144}\pi^2 - \frac{9}{4}\zeta(3)\right) C_A + \left(\frac{1}{54} + \frac{1}{72}\pi^2\right) N_f\right]. \quad (4.6)$$

While  $\Gamma_{\text{cusp}}(g)$  is a universal number,  $\Gamma(g)$  depends on the path under consideration. The unusual feature of the RG equation (4.5) is that the anomalous dimension given by the coefficient of  $W(C_S)$  in the r.h.s. depends on  $\rho$ , *i.e.* on the renormalization point  $\mu$  and  $y_-$ . Actually this property leads to the evolution equation for the structure function as we shall discuss in the next section.

## 5. Evolution equations

The RG equation for the distribution function near the phase space boundary is obtained by using the representation (2.12) and properties (2.22) and (2.23). Introducing the dimensionless parameter  $\sigma = (Py)$  we can write

$$F(x, \mu/M) = H(\mu/M) \int_{-\infty}^{\infty} \frac{d\sigma}{2\pi} e^{i\sigma(1-x)} W(\sigma\mu/M - i0) \quad (5.1)$$

with the inverse transformation

$$H(\mu/M) W(\sigma\mu/M - i0) = \int_{-\infty}^1 dx e^{-i\sigma(1-x)} F(x, \mu/M),$$

where the range of  $x$ -integration takes into account the spectral property of the structure function in (3.8). The renormalization group equation in (4.5) gives

$$\mathcal{D} F(x, \mu/M) \equiv \left(\mu \frac{\partial}{\partial \mu} + \beta(g) \frac{\partial}{\partial g}\right) F(x, \mu/M) = \int_x^1 dz P(1+x-z) F(z, \mu/M) \quad (5.2)$$

where

$$P(z) = \int_{-\infty}^{\infty} \frac{d\sigma}{2\pi} e^{i\sigma(1-z)} \{-2\Gamma_{\text{cusp}}(g) \ln[i(\sigma\mu/M - i0)e^{\gamma_E}] - \Gamma(g) + \mathcal{D} \ln H(\mu/M)\} .$$

From the analytical property of the integrand we have

$$P(z) = 0 \quad \text{for } z > 1 ,$$

this is the reason for setting to  $x$  the lower limit for  $z$  in (5.2). To compute  $P(z)$  we use the representation

$$\ln \rho = \int_0^{\infty} \frac{d\alpha}{\alpha} (e^{-\alpha} - e^{-\alpha\rho}) .$$

After a careful treatment of the  $\alpha \rightarrow 0$  singularities, we obtain

$$P(z) = 2\Gamma_{\text{cusp}}(g) \left( \frac{\theta(1-z)}{1-z} \right)_+ + \delta(1-z)h(g) \quad (5.3)$$

where  $(\dots)_+$  is the standard plus-distribution and

$$h(g) = -\Gamma(g) + 2\Gamma_{\text{cusp}}(g) \ln \frac{M}{\mu} + \mathcal{D} \ln H(\mu/M) . \quad (5.4)$$

Due to the factorization theorem [9],  $P(z)$  should not depend on  $\mu$  and the same is then true for the function  $h(g)$ . This means that the  $\mu$  dependence in the term involving the coefficient function  $H(\mu/M)$  should be compensated by a contribution from  $W(C_S)$ . One can consider now (5.4) as the RG equation for the function  $H(\mu/M)$ . While only soft gluons contribute to  $\Gamma_{\text{cusp}}(g)$ , both soft and collinear gluons (and quarks) contribute to  $h(g)$ . Therefore the function  $h(g)$  is not fixed by the RG equation of  $W(C_S)$  and should be directly computed [18] from Feynman diagrams.

Notice that the function  $F(x, \mu/M)$  defined in (5.1) satisfies the evolution equation (5.2) for any value of  $x$ . However, this function has the physical meaning of the quark distribution only for  $x \rightarrow 1$ .

The evolution equation (5.2) in the soft limit  $x \sim 1$  and  $z \sim 1$  can be written in the standard form (4.1) where  $P(z)$  is the two-loop quark splitting function for  $z$  near 1. From (5.3) the general form of  $P(z)$  is given by

$$(1-z)P(z) = 2\Gamma_{\text{cusp}}(g) \theta(1-z) . \quad (5.5)$$

Using the expression (4.3) for  $\Gamma_{\text{cusp}}(g)$  one easily verifies that the result of two-loop calculations [18] obeys this relation.

The evolution equation (5.2) for  $x \sim 1$  is obtained from the RG equation for the light-like Wilson loop. Because of the universal structure of RG equation, one finds that any distribution, which can be represented in terms of the light-like Wilson loops, satisfies equation (5.2) with the kernel  $P(z)$  defined by (5.5). This is the case for the quark and gluon structure and fragmentation functions (see subsect. 2.3) at large  $x$ . For the gluon distributions one should replace the colour factor  $C_F$  by  $C_A$  in (4.3).

Let us consider the moments of the function  $F(x, \mu/M)$  defined in (5.1),

$$F_n(\mu/M) = \int_0^1 dx x^{n-1} F(x, \mu/M) = H(\mu/M) \int_0^1 dx x^{n-1} \int_{-\infty}^{\infty} \frac{d\sigma}{2\pi} e^{i\sigma(1-x)} W(\sigma\mu/M - i0) . \quad (5.6)$$

For large  $n$  the integral over  $x$  receives the leading contribution from the  $x \rightarrow 1$  region in which  $F(x, \mu/M)$  coincides with the quark distribution function. By using the two-loop expression for  $W(\sigma\mu/M - i0)$  in (3.7) we obtain the corresponding  $F_n(\mu/M)$ . Before this we note that  $W(\sigma\mu/M - i0)$  is given to any order in perturbation theory by a sum of powers of  $L = \ln[i(\sigma\mu/M - i0)] + \gamma_E$ . Hence, in order to find  $F_n(\mu/M)$  one needs to expand the following basic integral

$$\int_0^1 dx x^{n-1} \int_{-\infty}^{\infty} \frac{d\sigma}{2\pi} e^{i\sigma(1-x)} \left[ i \left( \sigma \frac{\mu}{M} - i0 \right) \right]^{-\delta} = \left( \frac{\mu}{M} \right)^{-\delta} \frac{\Gamma(n)}{\Gamma(n+\delta)} = \left( \frac{\mu}{M} n \right)^{-\delta} (1 + \mathcal{O}(1/n)),$$

in powers of  $\delta$ . This relation implies that for large  $n$  and arbitrary  $\delta$  the integral is given by the integrand evaluated at  $\sigma = -in$ . Performing this trick in (5.6) we get the simple expression

$$F_n(\mu/M) = H(\mu/M)W(-in\mu/M) (1 + \mathcal{O}(1/n)), \quad (5.7)$$

which means that the large- $n$  behavior of the moments of the quark distribution function is given by the Wilson loop expectation value evaluated along the path of fig. 2 with formal identification  $(Py) = -in$  (or  $\rho = -in\mu/M$ ) in (2.22) and (2.23). From (5.7) and the non-abelian exponentiation theorem we obtain that large- $n$  corrections to  $F_n$  exponentiate. From the one- and two-loop results in (2.21) and (3.7) we get that the exponent of  $F_n$  contains a sum of powers of  $\ln n$  up to  $\alpha_s \ln^2 n$  terms in one loop and  $\alpha_s^2 \ln^3 n$  terms in two loops. The sum of all these corrections to all orders can be done by using the RG equation (4.5) for light-like Wilson loops. From this equation and from (5.7) we find that the large- $n$  behaviour of  $F_n(\mu/M)$  is governed by

$$\left( n \frac{\partial}{\partial n} + \beta(g) \frac{\partial}{\partial g} \right) F_n(\mu/M) = - [2\Gamma_{\text{cusp}}(g) \ln(ne^{\gamma_E} \mu/M) + \Gamma(g)] F_n(\mu/M). \quad (5.8)$$

To test the relation (5.7) we differentiate  $F_n(\mu/M)$  w.r.t.  $\mu$  and substitute eqs. (4.5) and (5.4) to obtain

$$\left( \mu \frac{\partial}{\partial \mu} + \beta(g) \frac{\partial}{\partial g} \right) F_n(\mu/M) = - [2\Gamma_{\text{cusp}}(g) \ln(ne^{\gamma_E}) - h(g)] F_n(\mu/M). \quad (5.9)$$

One easily checks that the same equation follows from (5.2) with the l.h.s. equal to the moment of the evolution kernel (5.3) for large  $n$ .

## 6. Concluding remarks

To conclude we would like to mention a close relation between the analysis here presented and the heavy quark effective field theory (for a review see ref. [19]) which seems to be a powerful tool for analyzing of heavy meson phenomenology. The emission of gluons from heavy quarks can be treated by the eikonal approximation. This implies that the propagation of the heavy quarks through the cloud of light particles can be described by Wilson lines and that the effective heavy quark field theory can actually be formulated [20] in terms of the Wilson lines. Therefore, the renormalization properties of Wilson lines discussed in this paper are related to the ones for the effective theory. For example one finds that the “velocity dependent anomalous dimension” is the cusp anomalous dimension (4.3).

The central point of our analysis was the RG equation (4.5) for the generalized Wilson loop expectation value,  $W(C)$ , with path partially lying on the light-cone. The cusp anomalous dimension  $\Gamma_{\text{cusp}}(g)$  entering into this equation is a new universal quantity of perturbative QCD



which controls the behaviour near the phase space boundary of hard distributions. The evolution equation for these distributions corresponds to the RG group equation for  $W(C)$ , moreover the splitting function near the phase space boundary is related to the cusp anomalous dimension. This equation does not imply that  $W(C)$  is renormalized multiplicatively.

It is well known that the structure function of deep inelastic scattering gets large perturbative corrections for  $x \rightarrow 1$  which need to be summed [2, 3]. They come from two subprocesses: from quark distribution function and from cross section of the partonic subprocess. In the present paper we considered the  $x \rightarrow 1$  behavior of the distribution functions. We were able to control in eqs. (5.8) and (5.9) their large perturbative corrections to all orders using the renormalization properties of light-like Wilson loops. The same method can be applied for the summation of large perturbative corrections to the partonic cross section [2, 3]. It will be described in the forthcoming paper.

## Note added on February 4, 2005

Recently the two-loop calculation of the Wilson loop  $W(C_S)$  has been performed by E. Gardi in ref. [21]. The obtained results for the Feynman integrals  $I_1, \dots, I_{10}$  agree with our expressions while  $I_{11}$  differs by  $\sim 1/(D-4)$  term. We repeated the calculation of  $I_{11}$  and reproduced the result of [21]. In the present version, we updated expressions for the integral  $I_{11}$ , Eq. (3.6), the  $D$ -coefficient, Eq. (3.7) and the anomalous dimension  $\Gamma(g)$ , Eq. (4.6), by taking into account the contribution of the additional term.

We are most grateful to E. Gardi and M. Neubert for useful discussions and correspondence.

## Appendix A: Feynman rules in the coordinate representation

In this appendix we recall the Feynman rules for calculation the generalized Wilson loop expectation value in the coordinate representation using dimensional regularization. The  $D$ -dimensional free gluon propagator in the Feynman gauge is given by  $D^{\mu\nu}(x) = -g^{\mu\nu}D(x)$  where

$$D(x) = i \int \frac{d^D k}{(2\pi)^D} e^{-ikx} \frac{1}{k^2 + i0} = \frac{\Gamma(D/2 - 1)}{4\pi^{D/2}} (-x^2 + i0)^{1-D/2}$$

The ‘‘cutted’’ propagator  $D_+^{\mu\nu}(x) = -g^{\mu\nu}D_+(x)$  associated to a real gluon is defined as

$$D_+(x) = \int \frac{d^D k}{(2\pi)^D} e^{-ikx} 2\pi\theta(k_0)\delta(k^2) = \frac{\Gamma(D/2 - 1)}{4\pi^{D/2}} [-2(x_+ - i0)(x_- - i0)]^{1-D/2}$$

where the last equality holds only for  $\mathbf{x}_T = 0$ . We note that for gluon propagating in the time-like direction ( $x_+ > 0$ ,  $x_- > 0$  and  $\mathbf{x}_T = 0$ ) cutted and full propagator coincide. For the three-gluon vertex with three gluon propagators attached we have

$$\begin{aligned} & \Gamma_{\mu_1\mu_2\mu_3}(z_1, z_2, z_3) \int d^D z_4 \prod_{i=1}^3 D(z_4 - z_i) \\ &= -i (g^{\mu_1\mu_2} (\partial_1^{\mu_3} - \partial_2^{\mu_3}) + g^{\mu_2\mu_3} (\partial_2^{\mu_1} - \partial_3^{\mu_1}) + g^{\mu_1\mu_3} (\partial_3^{\mu_2} - \partial_1^{\mu_2})) \int d^D z_4 \prod_{i=1}^3 D(z_4 - z_i) \end{aligned}$$

For the gluon attached to the point on the ray  $\ell_1$  of the integration path of fig. 2 and propagating to  $z$  we have  $igv_\mu \int_{-\infty}^0 dt_1 D(vt_1 - z)$ . The analogous expressions for a gluon attached to the segment  $\ell_2$  and the ray  $\ell_3$  are  $igy_\mu \int_0^1 dt_2 D(yt_2 - z)$  and  $-igv_\mu \int_0^\infty dt_3 D(y - vt_3 - z)$  respectively.

The scalar products and integration measure in terms of light-cone variables are

$$a_\pm = \frac{1}{\sqrt{2}}(a_0 \pm a_3), \quad \mathbf{a} = (a_1, a_2), \quad (ab) = a_+b_- + a_-b_+ - \mathbf{a} \cdot \mathbf{b}, \quad d^D a = da_+ da_- d^{D-2} \mathbf{a}$$

for arbitrary  $D$ -dimensional vectors  $a_\mu$  and  $b_\mu$ .

## References

- [1] A.H.Mueller, Phys. Rep. 73 (1981) 237;  
G.Altarelli, Phys. Rep. 81 (1982) 1;  
A. Bassetto, M. Ciafaloni and G. Marchesini, Phys. Rep. 100 (1983) 201;  
Yu.L. Dokshitzer, V.A. Khoze, A.H. Mueller and S.I. Troyan, Rev. Mod. Phys. 60 (1988) 373; *Basics of Perturbative QCD*, Editions Frontières, Paris, 1991.
- [2] G.Sterman, Nucl. Phys. B281 (1987) 310.
- [3] S.Catani and L.Trentadue, Nucl. Phys. B327 (1989) 323; B353 (1991) 183.
- [4] G.Parisi, Phys. Lett. B90 (1980) 295;  
G.Curci and M.Greco, Phys. Lett. B92 (1980) 175.
- [5] W.L. van Neerven, Phys. Lett. B147 (1984) 175.
- [6] S.Catani and M.Ciafaloni, Nucl. Phys. B236 (1984) 61; B249 (1985) 301;  
S.Catani, M.Ciafaloni and G.Marchesini, Nucl. Phys. B264 (1986) 558.
- [7] S.V.Ivanov and G.P.Korchensky, Phys. Lett. B154 (1985) 197; *in Proc. Quarks 84*, Tbilisi, 1984, Vol.2, p.145.
- [8] V.N.Gribov and L.N.Lipatov, Yad. Fiz. 15 (1972) 781; 1218;  
L.N.Lipatov, Yad. Fiz. 20 (1974) 181;  
G.Altarelli and G.Parisi, Nucl.Phys. 126B (1977) 298.
- [9] J.C.Collins, D.E.Soper and G.Sterman, "Factorization of Hard Processes in QCD," in "Perturbative Quantum Chromodynamics", ed. by A.H.Mueller (World Scientific, Singapore, 1989) p.1.
- [10] J.C.Collins and D.E.Soper, Nucl. Phys. B194 (1982) 445.
- [11] T.Kinoshita, J.Math.Phys. 3 (1962) 650;  
T.D.Lee and M.Nauenberg, Phys.Rev. 133 (1964) 1549.
- [12] G.Sterman, Phys. Rev. D17 (1977) 2773.

- [13] A.M.Polyakov, Nucl. Phys. B164 (1980) 171;  
I.Ya.Aref'eva, Phys. Lett. B93 (1980) 347;  
V.S.Dotsenko and S.N.Vergeles, Nucl. Phys. B169 (1980) 527;  
R.A.Brandt, F.Neri and M.-A.Sato, Phys. Rev. D24 (1981) 879.
- [14] J.G.M.Gatheral, Phys. Lett. 113B (1984) 90;  
J.Frenkel and J.C.Taylor, Nucl. Phys. B246 (1984) 231.
- [15] A.Andrasi and J.C.Taylor, Nucl. Phys. B350 (1991) 73.
- [16] I.A.Korchenskaya and G.P.Korchemsky, Phys. Lett. 287B (1992) 169.
- [17] G.P.Korchemsky and A.V.Radyushkin, Nucl. Phys. B283 (1987) 342.
- [18] G. Curci, W. Furmanski and R. Petronzio, Nucl. Phys. B175 (1980) 27;  
W. Furmanski and R. Petronzio, Z. Phys. C11 (1982) 293;  
J. Kalinowski, K. Konishi, P.N. Scharbach and T.R. Taylor, Nucl. Phys. B181 (1981) 253;  
E.G. Floratos, C. Kounnas and R. Lacaze, Phys. Lett. 98B (1981) 89;  
I. Antoniadis and E.G. Floratos, Nucl. Phys. B191 (1981) 217.
- [19] For a review see: H.Georgi, "Heavy Quark Effective Field Theory," preprint HUTP-91-A039 (1991).
- [20] G.P.Korchemsky and A.V.Radyushkin, Phys. Lett. 279B (1992) 359.
- [21] E.Gardi, arXiv:hep-ph/0501257.